Application of Carbon Fiber Paper in Integrated Wooden Electric Heating Composite

Quanping Yuan and Feng Fu*

To endow wooden material with an electric heating function, carbon fiber paper, as an electric heating membrane, was laminated with wood veneer to prepare wooden electric heating composites. The electric heating performance of the membrane under different power densities and resistance stabilities, as well as the influencing mechanism of the process on both the resistance and bonding performance of the composite, were studied. The surface temperature of the membrane and composite increased by more than 20 °C in 30 s and 10 min, respectively, after electricity was applied. Furthermore, the samples had a surface temperature unevenness of 4 and 2 °C, respectively. Many potential contact points between carbon fibers fulfilled their connections, reducing the drop rate of resistance (DRR) after hot-pressing to the range of 30% to 43%. The hot-press pressure and glue spread had a high degree of relevancy (coefficient of determination R^2=0.960 and R^2=0.997) with the DRR of the composite, respectively. The composite exhibited a negative temperature coefficient effect (NTC), and the DRR after heating for 15 h was 4.4%, but tended to ultimately stabilize. The composite, which exhibited good time-temperature effects and had a linear relationship with a high value of the coefficient of determination (R^2=0.983) between power density and equilibrium temperature, displays solid potential for use in preparing integrated wooden electric heating products.

Keywords: Electric heating; Wooden composite; Carbon fiber paper; Integration; Negative temperature coefficient effect

Contact information: Research Institute of Wood Industry, Chinese Academy of Forestry; Key Lab of Wood Science and Technology of State Forestry Administration, Beijing 100091, P. R. China;
** Corresponding author: feng@caf.ac.cn*

INTRODUCTION

Low-temperature floor systems are becoming increasingly popular for use in indoor heating (Qi *et al.* 2012). Examples include hot water-heated floor systems (Obata *et al.* 2003; Seo *et al.* 2011), electric heating cable floor systems (Armstrong 1978; Selvais 2004), and electric heating membrane systems (Sun *et al.* 2008; Li *et al.* 2009). With the increasing concern regarding energy conservation and carbon dioxide emissions, an electric heating system is desirable due to its clean and highly efficient electric power source, while hot water-heated floor systems depend on carbon emission-intensive coal, natural gas, and other fossil fuel sources. Additionally, hot water heating systems also have lower thermal conversion rates.

Currently, electric heating systems are composed of a thick combination of an electric heating element on the bottom of the system and a floor layer on the upper portion (Lin and Zhang 2003). Among the materials typically used in the construction of the floor, wood has numerous advantages such as even temperature distribution (Qi *et al.* 2012), good tactile warmth (Obata *et al.* 2003), excellent appearance, and high latent heat.

Therefore, wood is the most common cover layer for floor heating systems (Seo *et al.* 2011). However, the thermal conductivity of wood flooring layers, in a given range of thicknesses, tends to be very low, ranging from 0.091 to 0.125 W/m·K (Seo *et al.* 2011). Wood's thermal conductivity in this range is very similar to that of heat insulation materials, which causes consumer concerns (Seo *et al.* 2011). Mou (2007) tested the heating performance of an electric heating system composed of an insulation layer placed under a carbon fiber electric heating membrane and laminate flooring (thickness of 12 mm) used as the cover layer. The results of the studied electric heating system showed that the temperature on the surface of the flooring increased by 20 °C and stabilized after being subjected to 40 min of heating. Furthermore, the system's overall power declined throughout the course of the process, from about 949 to 353 W/m^2. The thermal transfer rate was thus relatively low, considering the high power density for the thick flooring above, and the power showed large variations. Therefore, research for improvement on this deficiency, as well as other wooden flooring with high thermal transfer rates, is urgently needed.

Moreover, in terms of the electric heating element, carbon material exhibits a rapid temperature response and high electrothermal conversion efficiency (Jeon and Jeong 2013). Compared to carbon black (Enríquez *et al.* 2014), graphite, and carbon nanotubes (Jeon and Jeong 2013), carbon fiber exhibits a lower filling amount threshold value when it is applied to prepare a conductive composite (Wang *et al.* 2002) and is more suitable for heating composites. The electrothermal conversion efficiency of carbon fiber, in which radiation thermal conduction in the form of infrared wavelength ranges from 2.5 to 13 μm and can provide health benefits to humans, is above 90% (He 2005). However, research focused on carbon fiber applications in wooden material has mostly concentrated on reinforcement (Khan *et al.* 2013) and electromagnetic shielding (Yuan *et al.* 2013). For practical applications, chopped carbon fiber with wooden fibers has been used during the process of papermaking to produce facial electric heating paper. Such paper was then used to prepare a facial heating sheet that exhibits NTC or PTC (positive temperature coefficient), good linear correlation between power and surface temperature, stable power under long-term working, and a large-area property (Yang *et al.* 2000). Moreover, the resistance of carbon fibers has an important relationship with input power for electric heating, which needs to be accurately controlled after hot-pressing for practical applications.

Consequently, to shorten the thermal transfer distance to the heating surface and improve the thermal conductivity of the electric heating system, carbon fiber paper (CFP) with good electric heating performance and even distribution of carbon fibers was laminated onto wooden material to prepare an integrated wooden electric heating composite. This process will have important implications for making electric heating wooden floors and wallboards with high efficiency and reduced thickness.

EXPERIMENTAL

Materials

Eucalyptus veneer, with an average thickness of 2.4 mm, was air-dried to a moisture content between 7 to 9% and cut into 250 mm × 250 mm pieces. The CFP, with surface density of 60 g/m^2, a square resistance of 40 Ω, and a thickness of 0.12 mm was supplied by the Beijing Beyond Special Materials Co. Ltd. (China). Modified ureaformaldehyde (UF) resin adhesive powder (weight ratio of powder UF (C505) to modifier (M356), curing agent (H271), and water; 100:15:15:60) was provided by Boshijiao Fendeli Adhesive Co. Ltd. (China). The copper foil electrode, 10-mm width and 0.02-mm thick, was made in the lab.

Methods

Preparation of integrated wooden electric heating composite

The CFP was first cut into 250 mm × 250 mm pieces, and two electrodes were pasted on two sides of the sample, at a distance of 200 mm, to produce the electric heating membrane. After three layers of veneer were coated with glue and the one-layer membrane was embedded in one glue layer, the laminated structure (Fig. 1) was completed.

Single-factor testing was used to study the process. Plate temperature and hot-press time were set at 110 °C and 1.2 min/mm, based on preliminary tests. When testing the effect of hot-press pressure on the composite, glue spread was fixed at 280 g/m^2 and the composite was formed using hot-press pressures of 1.0, 1.2, 1.4, 1.6, and 1.8 MPa. When testing the effect of glue spread, the pressure was fixed at 1.2 MPa and double-sided glue spreads of 180, 230, 280, 330, and 380 g/m^2 were adopted to prepare the composite.

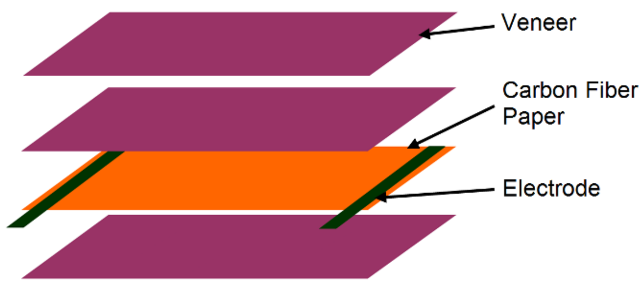

Fig. 1. Structure of wooden electric heating composite (the surface furthest from the carbon fiber paper was the surface used for temperature testing)

Micro-distribution of carbon fiber before and after bonding

The micro-distribution of carbon fibers in the paper was observed using an S-4800 scanning electronic microscope (SEM; Hitachi; Japan) operating at an accelerating voltage of either 10 kV or 20 kV. Samples approximately 3 mm × 3 mm were prepared, to include CFP before bonding and the CFP bonding layer inside the composite (both parallel and perpendicular to the glue layer). The samples were each mounted on a stub with double-sided conductive tape and sputter-coated with a gold alloy.

Bonding performance test

The bonding strength of the composite was tested according to the Chinese standard GB/T 9846 (2004) for type II plywood. The specimen was first soaked in water at 63±3 °C for 3 h, then left to cool for 10 min at room temperature. Finally, a WDW-W universal mechanical testing machine (Jinan Shidai Shijin Yiqi Co., Ltd.; China) was used to test the bonding strength of the specimen and the wood failure ratio. Wood failure ratio is defined as the percentage of wood failure area relative to the total shear area. The value of the ratio is used for the assist assessment of the bonding performance. The larger the wood failure ratio is, the better will be the bonding performance.

Drop rate of resistance (DRR) test

The resistance of the CFP, both before and after hot-pressing or application of electricity, was tested using a TH2512 low-resistance testing instrument (Changzhou Tonghui Electronics Co., Ltd.; China). The DRR is defined as the percentage difference between the resistance before and after hot-pressing or application of electricity.

Two wooden pad strips were placed above the electrode and below the CFP (corresponding to the electrode) and compressed with a C- clamp to impinge on the paper. The applied pressure was determined by that the value of testing resistance did not change with an increase in pressure. Finally, the low-resistance tester was used to test the resistance by connecting to the electrodes. The resistance of the sample after being hot-pressing was also measured.

Electric heating performance test

For the purpose of this study, room temperature was determined to be 22.5 °C. In this stage, the two electrodes on the carbon fiber electric heating membrane were subjected to a certain pressure to impinge on the paper (similar to the method described previously) and connected to a DH1719A-2 DC power source (Beijing Dahua Electronic Group; China) at a power density of 500 W/m^2. The temperature at points A, B, and C (Fig. 2) was measured every 20 s with a UT300A infrared temperature tester (resolution of 0.1; distance and light spot diameter ratio as 10:1; Uni-Trend Group Ltd.; Dongguan, China). The vertical distance between the tester and testing point was 100 mm. The average value of the three points was used as the final temperature value. The temperature distribution on the surface was tested after reaching a thermal balance (the surface temperature remains stable, since the generated heat is basically equal to the heat transmitted to the air) based on the temperature testing diagram (Fig. 2). It should be noted that power density defines only the power *per* valid electric heating area (*i.e.*, the area between two electrodes).

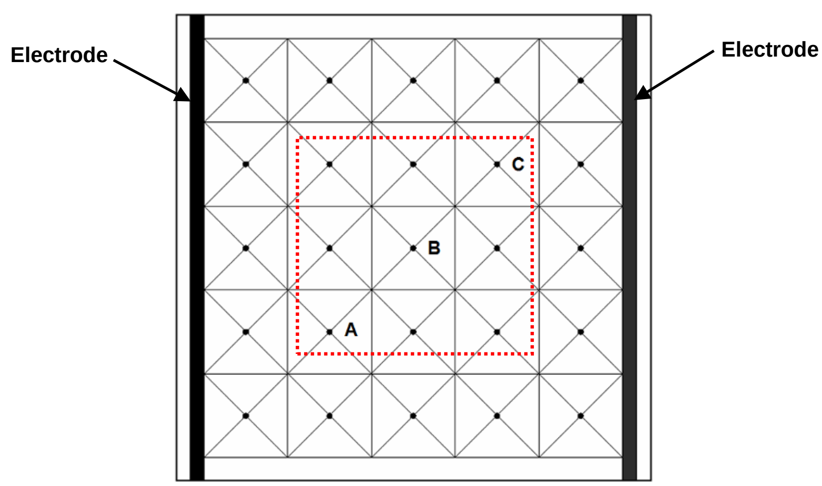

Fig. 2. Testing figure for temperature distribution. The test points result from the intersection of the line connecting the equipartition points. A 25 mm margin was set apart on both sides along the length of the electrodes

After the electric heating composite was connected to the DC power source, the following power densities were applied by controlling output voltage: 100, 200, 300, 400, and 500 W/m^2. During the power density application, the temperature (every 2 min) and the distribution after equilibrium were measured based on the method above. In addition, the resistance with an increase in heating time was recorded.

In Fig. 2, the uneven temperature is defined by the difference between the maximum and minimum value among the nine points in the center (as denoted by the red box).

Data analysis

Following the tests, a correlation of hot-press pressure and glue spread with DRR was fit using OriginPro v8.0 (OriginLab Corporation; USA) to find trends for DRR. In addition, the correlation between power density and equilibrium temperature was also fit to indicate a trend for electric-heating temperature. A linear and Gaussian fit was run at a 95% confidence level and equations generated along with the coefficient of determination (R^2) to judge the fitting precision.

RESULTS AND DISCUSSION

Electric Heating Performance of Carbon Fiber Membrane

It can be seen in Fig. 3 that the carbon fiber membrane exhibited a rapid temperature response, rising by more than 20 °C in 30 s. The performance of the carbon fiber membrane resulted from its heat transmitting mechanism. The heat transfer of carbon fiber mainly depends on thermal radiation conducting to another medium (*i.e.*, wood fiber and air surrounding the carbon fiber), by which the heat induced by electric current can dissipate quickly.

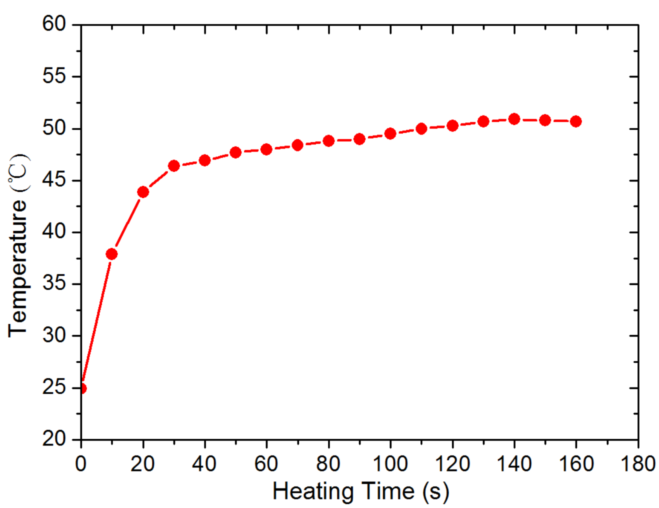

Fig. 3. Electric heating performance of carbon fiber paper (power density of 500 W/m²)

Carbon fiber is a good heat conductor, which depends on lattice vibrations (*i.e.*, phonons). As the average free path of the phonon in carbon fibers increases, the thermal conductivity increases (He 2005). Carbon fiber has the proper number of phonons with a sufficient average free path after carbonized at a temperature as high as 1500 °C during its preparation process (Yang *et al.* 2000). Therefore, carbon fiber has a very high heat transfer efficiency. Moreover, because they possess a large surface area and an average diameter of about 7 μm, carbon fibers can dissipate heat rapidly after electricity is applied, leading to a low thermal storage and no local overheating (Yang *et al.* 2000). Consequently, the temperatures of the membrane reached only about 50 °C when subjected to a high power density of 500 W/m^2. The three-dimensional conductive net structure made of carbon fiber and wood fiber, shown in Fig. 4, was also conducive to the dissipation of thermal energy.

Figure 5 shows that the temperature distribution on the membrane varied at different points. After calculations were performed, the overall temperature unevenness was determined to be 4 °C, resulting from the variable distribution of carbon fibers (Fig. 4). At a microscopic level, carbon fibers in the membrane can migrate; however, the unevenness was only 4 °C, further demonstrating the carbon fibers have high thermal transfer and dissipation rates.

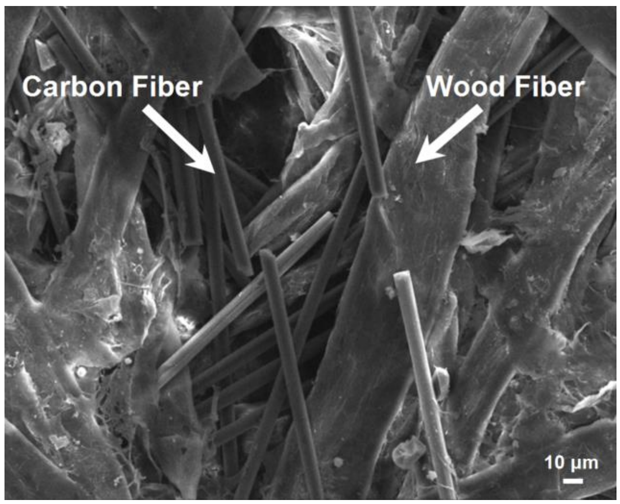

Fig. 4. SEM image of the electric heating membrane

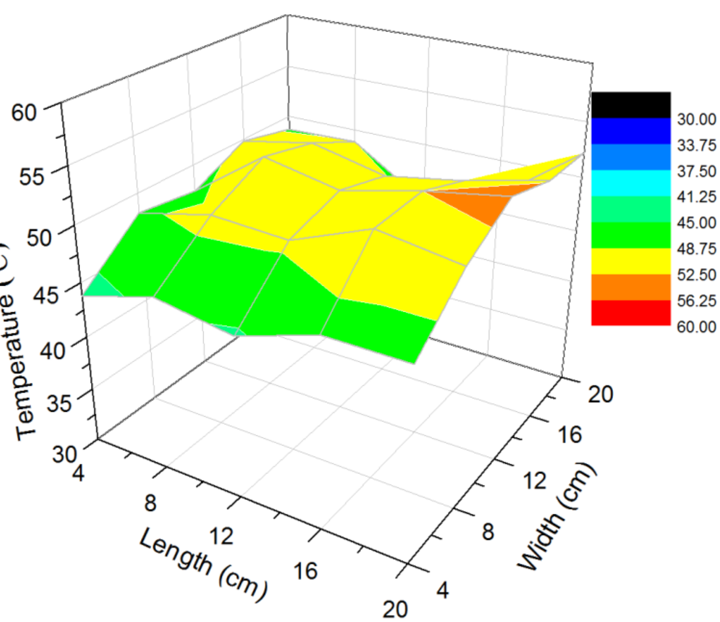

Fig. 5. Temperature distribution on electric heating membrane (power density of 500 W/m^2)

Influence of Process on DRR

Figures 6 and 7 show that DRR content can reach a maximum of 43% and a minimum of 30% at pressures ranging from 1.0 to 1.8 MPa and glue spread ranging from 180 to 380 g/m^2. The results are due to the fact that carbon fibers come into contact with other carbon fibers distributed at the potential contact points. The contact points are grouped more closely during bonding (Fig. 8) and the conductive network is further improved.

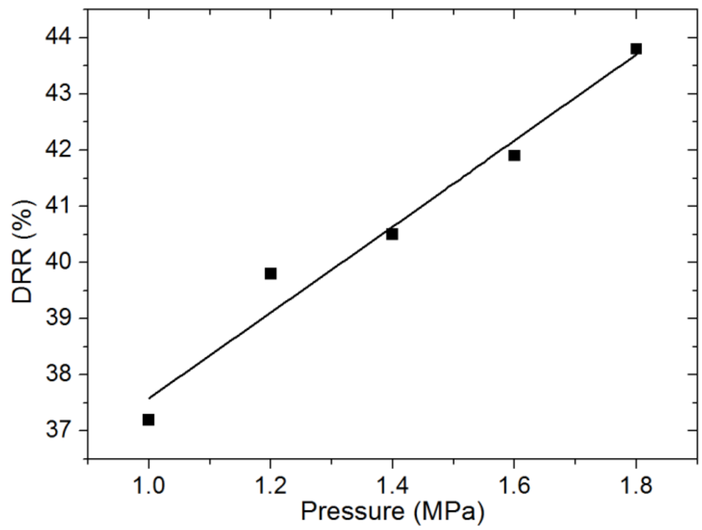

Fig. 6. Relationship between hot-press pressure and DRR

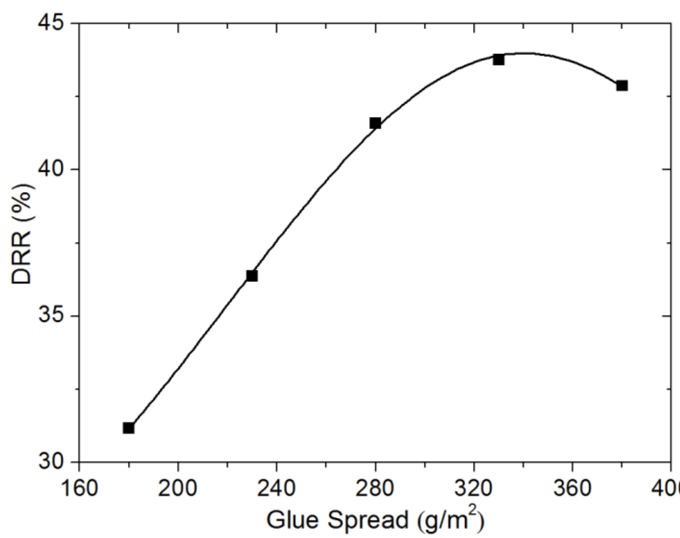

Fig. 7. Relationship between glue spread and DRR

It was found that the relationship between pressure and DRR showed good correlation *via* linear fitting (Eq. 1, R^2= 0.960). Increasing the pressure also increased the potential contact points and the contact area, while decreasing the contact resistance between contacted fibers and the resistance of the total conductive structure (Fig. 8). The DRR at pressures of 1.2 to 1.6 MPa was found to be the most stable, and its range was less than 7%.

$$y = 29.93 + 7.65x \quad (1)$$

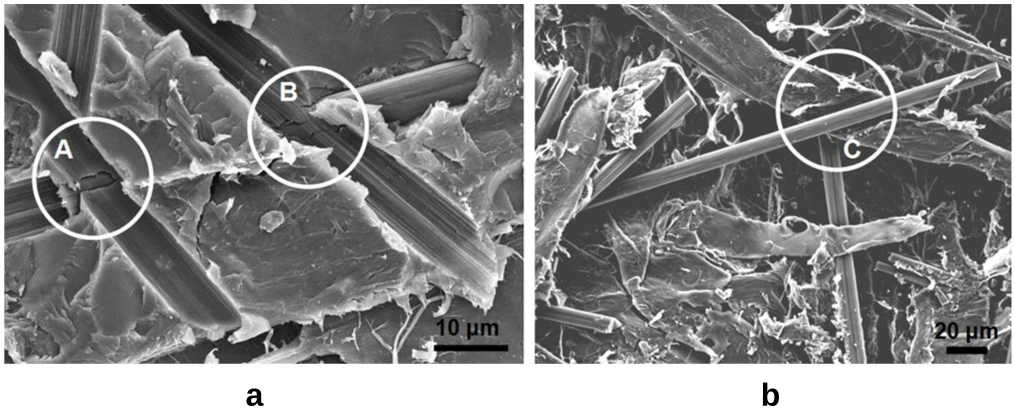

Fig. 8. SEM images showing potential contact points after pressing. (a) contact points among carbon fibers in close contact by adhesion; contacting points A and B show close contact, where the contacted carbon fibers have been separated when samples were prepared. (b) potential contact points after bonding, where carbon fibers come into contact with the fibers below, squeezing the wood fiber between them (*i.e.*, point C)

The range of glue spread was slightly greater than that of pressure, totaling less than 12%. The relationship between glue spread and DRR is an exponential function determined *via* nonlinear fitting (Eq. 2), with a high coefficient of determination (R^2=0.997). After a glue spread of 280 g/m^2 was applied, the DRR was more stable than that applied at a lower glue spread. The DRR showed a slight decrease, when applied at 380 g/m^2 compared to an application of 330 g/m^2. It can be determined from Fig. 9 that glue was wedged into the carbon fiber lapping joint structure with high spreading of the glue, reducing the contact area and force, which had a negative influence on the resistance. Consequently, the glue had a two-sided effect on the conductive network of CFP bonding layer depending on its dosage. In practical application, the DRR could be preliminarily predicted by this equation, which would be conducive to designing the input power of the composite in advance.

$$y = 22.182 + 21.816\exp(-2((x - 340.313)/240.333)^2) \quad (2)$$

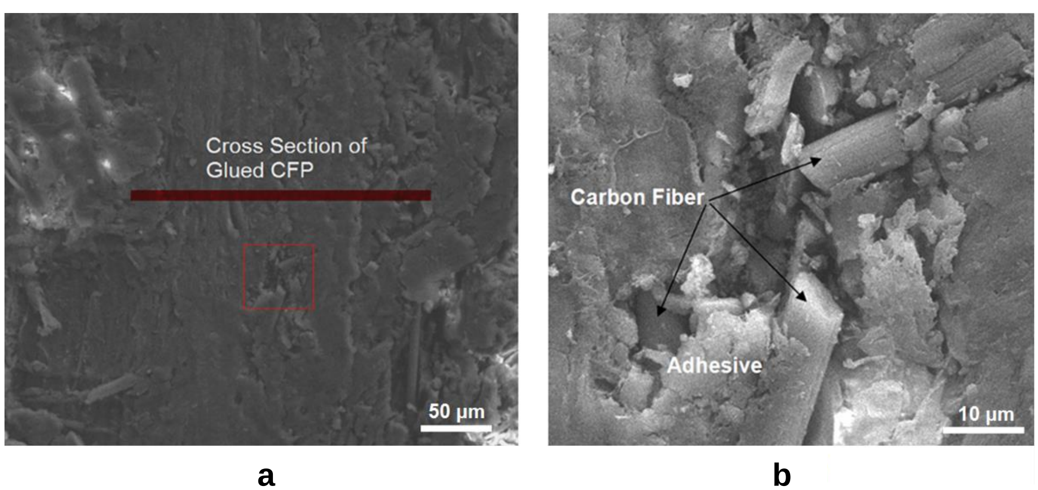

Fig. 9. SEM images of the electric heating layer in the composite with a glue spread of 380 g/m^2. (a) cross-section of electric heating layer and (b) distribution of glue among the conductive carbon fiber after bonding

Influence of Process on Bonding Performance

It is shown in Fig. 10 that the bonding strength of the upper portion of the sample reached 0.7 MPa, an adequate level according to the Chinese standard GB/T 9846 (2004) for type II plywood. Furthermore, the composite had a wood failure ratio of 45% when the pressure exceeded 1.2 MPa, at which point the DRR also leveled off. When exposed to a pressure greater than or equal to 1.8 MPa, the interlayer of the electric heating membrane became highly compacted, resulting in lower penetrability before the adhesive permeated into the composite during hot-pressing. The aforementioned process is the cause of the slight decrease in bonding strength when exposed to high pressure.

Figure 11 shows that the bonding strength of the composite reached 0.7 MPa on the upper portion, an adequate level according to the Chinese standard GB/T 9846 (2004) for type II plywood. The composite had a wood failure ratio of at least 40% when the glue spread exceeded 280 g/m^2, and it exhibited lower strength when exposed to a lower glue spread.

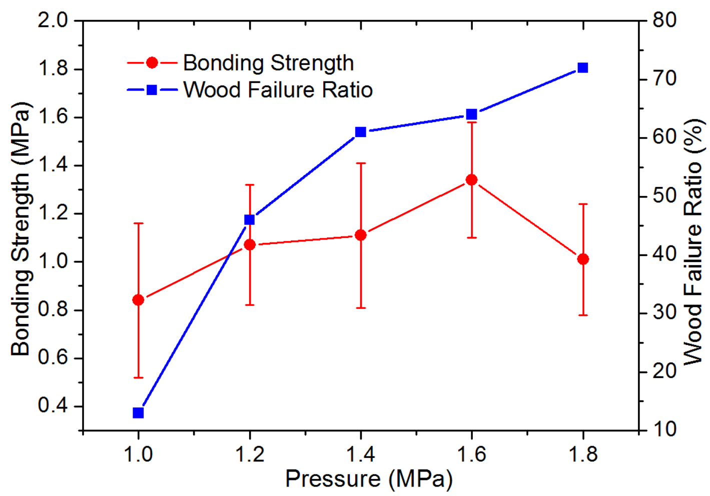

Fig. 10. Bonding strength at various pressures

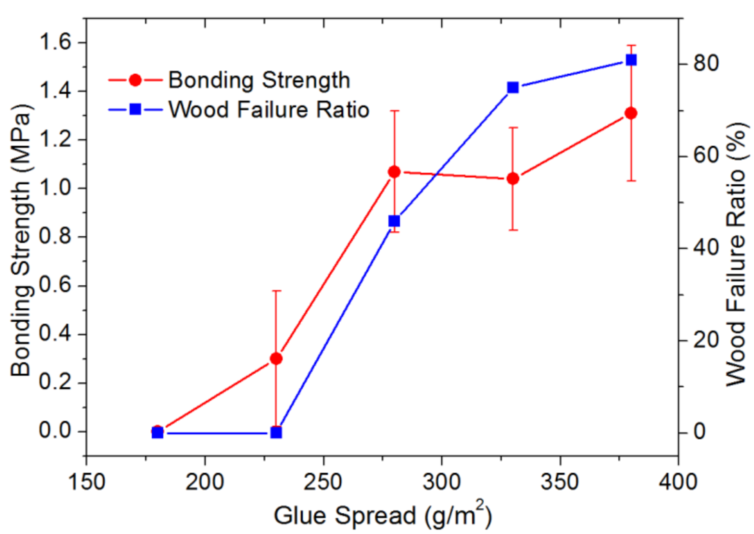

Fig. 11. Bonding strength at various glue spreads

Additionally, the sample had no strength when the glue spread was less than or equal to 180 g/m^2, as there was not enough adhesive permeating into the membrane. On the contrary, glue sufficiently filled the whole section with a high glue spread of 380 g/m^2, which contributed to the higher bonding strength and wood failure ratio (Fig. 9).

Electric Heating Performance of the Composite

Figure 12 indicates that the wooden electric heating composite had good time-temperature effects and automatic temperature control properties. When a power density of 500 W/m^2 was applied, the temperature increased by 20 °C on the surface in 10 min. Furthermore, as the applied power density increased, the time needed to reach an equilibrium temperature increased. The power density and equilibrium temperature had a highly linear relationship, as shown in Eq. (3), with a coefficient of determination (R^2) of 0.983, which is very useful for the practical application of setting the power with respect to target temperature (Fig. 13).

$$y = 23.3 + 0.057x \tag{3}$$

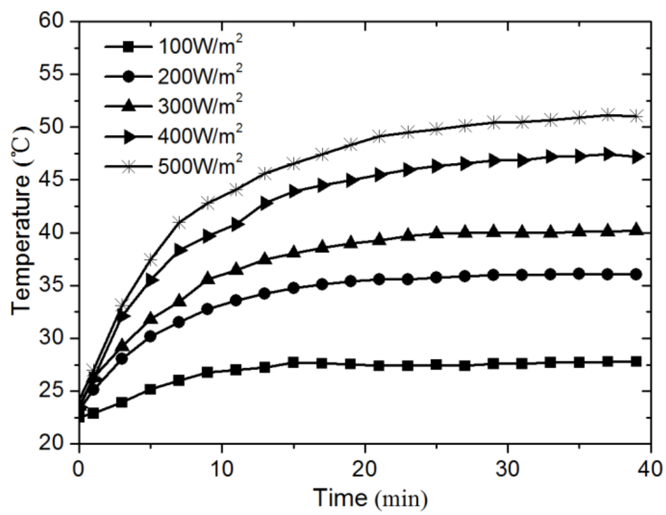

Fig. 12. Time-temperature effect of the composite at various power densities

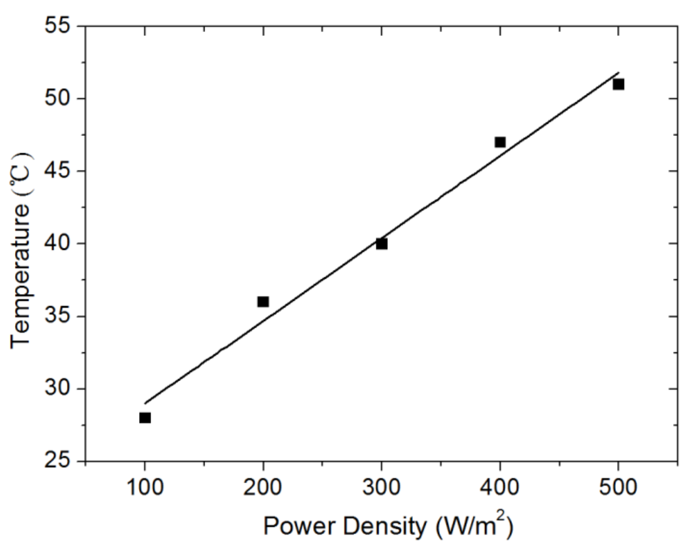

Fig. 13. Relationship between power density and equilibrium temperature

As shown in Fig. 14, the temperature distribution in the middle area of the panel surface was higher and more even than that at the margins because of the rapid thermal dissipation (Hua and Fu 1995). The thermal conductivity of wood along the longitudinal direction is far better than that in the transverse direction (Seo *et al.* 2011). In addition, the glue layer above the electric heating layer is a poor conductor of thermal energy. Both of these factors compel heat to be transmitted toward the edge of panel, creating relatively lower temperatures around the margin than around the center area. As can be seen in Table 1, the unevenness of the temperature distribution on the surface slightly increased with increasing power density. The unevenness of the temperature distribution was due to the rapid temperature response of the carbon fiber membrane generating heat immediately after becoming electrified within the interlayer (Fig. 3) as well as the composite's poor conductivity, which can result in higher temperatures in the middle area and lower temperatures around the edge. However, subjected to the highest power density of 500 W/m^2, the composite's unevenness value was only 2 °C, which is smaller than that of a plywood composite laminated with conductive adhesive (Hua and Fu 1995).

Table 1. Temperature Unevenness in the Center of the Panel at Various Power Densities

Power Density (W/m^2)	Temperature Maximum (°C)	Temperature Minimum (°C)	Average Value (°C)	Unevenness Value (°C)
100	28.3	27.2	27.7	1.1
200	37.0	35.9	36.4	1.1
300	41.0	40.1	40.7	0.9
400	49.8	48.2	48.9	1.6
500	54.5	52.5	53.5	2.0

The fact that the temperature unevenness of the composite was smaller than that of the carbon fiber membrane before being pressed at the same power density indicates that wood has a uniform thermal conductivity (Figs. 14 (b) and (c)). When the thermal energy was transmitted to the wooden layer (with its longitudinal direction parallel to the plane), the thermal energy was conducted uniformly along the longitudinal direction (having better conductivity than that along the transverse) in advance before it was transmitted toward the transverse (*i.e.*, the surface of the heating panel). Additionally, the air in the cell cavity, with higher temperature conductivity (about two orders of magnitude greater than that of wooden material), contributed to the results as well.

The resistance of the carbon fiber composite used for electric heating decreased slightly with increasing heating time and temperature (*i.e.*, negative temperature coefficient effect (NTC)), which can be credited to the dielectric breakdown and tunnel conduction of the insulating material around the conductive matrix by the function of electric current shock (Yang *et al.* 2000). In addition, the contacted points among carbon fibers could form chemical crosslinking under the electro and thermal catalysis, except for the physical contact (Yang *et al.* 2000). This phenomenon can be observed in Fig. 15, where the resistance of the wooden electric heating composite declined more in the initial working period than it did in later periods, during which it gradually stabilized.

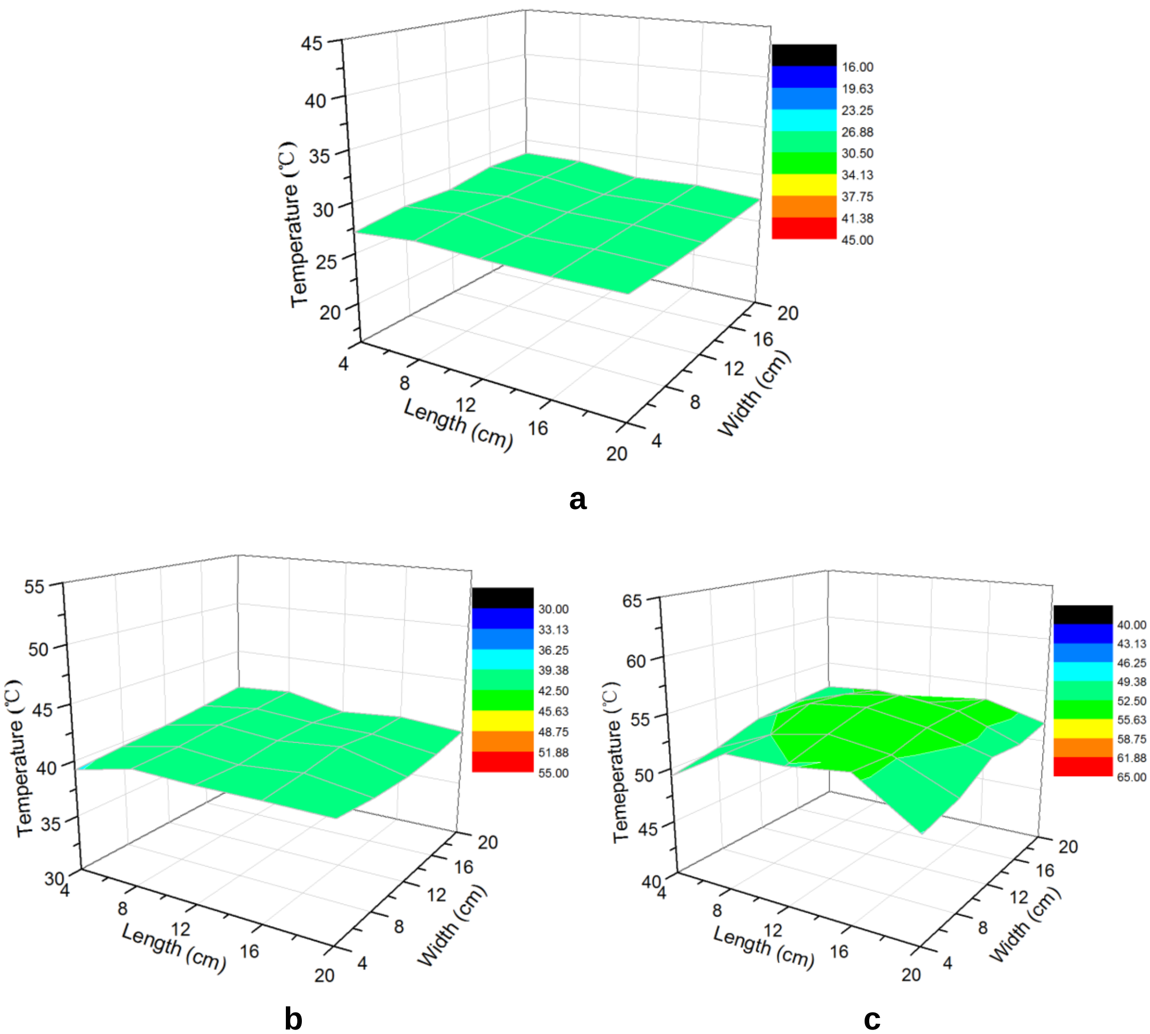

Fig. 14. Temperature distribution at different power density. (a) power density of 100 W/m^2. (b) power density of 300 W/m^2. (c) power density of 500 W/m^2

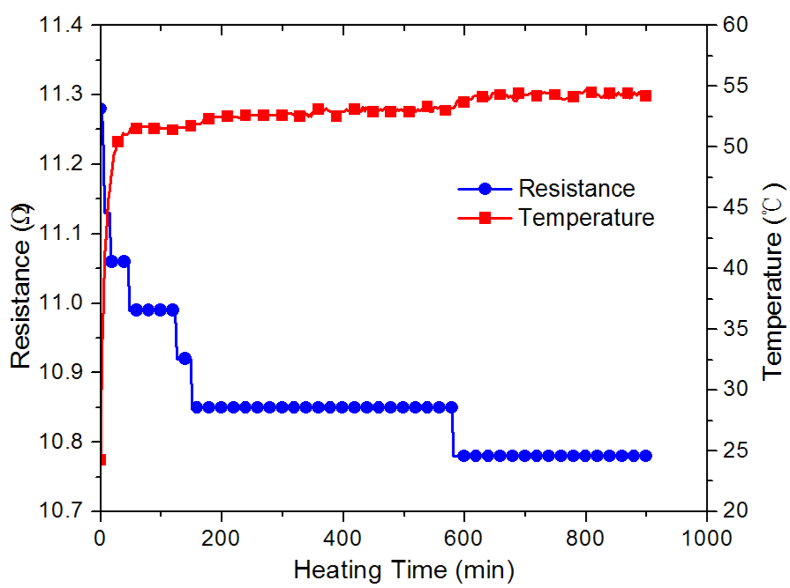

Fig. 15. Resistance of electric heating layer with increasing heating time

Generally, the power density in indoor wooden electric heating products is less than 300 W/m^2. When a power density of 500 W/m^2 was introduced in this test, the DRR (the percentage difference between the resistance before and after electrified) was 4.4% after electric heating for 15 h, supporting results found by Yang *et al* (2000) and suggesting that the composite was more stable than composites by Mou (2007). Simultaneously, the temperature kept changing in the process, because the applied power changed slightly for the dropped resistance after heating for a long time.

CONCLUSIONS

1. The surface temperature of a carbon fiber membrane was elevated by more than 20 °C after the initial 30 s of heating and that of the wooden electric heating composites was elevated by the same temperature after 10 min of heating, under a power density of 500 W/m^2, which indicates that both exhibited a rapid temperature response.
2. The bonding performance of the composite met the Chinese national standard GB/T 9846 (2004) for type II plywood when subjected to a pressure of 1.2 MPa and a glue spread of 280 g/m^2, and both had a high correlation with DRR (R^2=0.960 and R^2=0.997, respectively). The DRR can be controlled for carbon fiber paper within a wooden electric heating composite in terms of bonding and resistance.
3. The composite exhibited good time-temperature effects, and the equilibrium temperature had a significant linear relationship with power density (R^2=0.983). Furthermore, it was safe to use due to its automatic temperature control properties during electric heating.
4. The resistance of the composite declined less in the later working period than it did in the initial period, and the DRR was 4.4% under a power density of 500 W/m^2 after electric heating for 15 h. The composite exhibited a NTC effect in the initial working period, but a stable electric heating performance afterwards.
5. The composite had a lower surface temperature unevenness of 2 °C in the central area in comparison with the carbon fiber membrane. The low surface temperature unevenness indicates that the composite had uniform thermal conductivity, thus demonstrating its potential for application in wooden electric heating products.

ACKNOWLEDGMENTS

The authors are grateful for the support of the Special Fund for Forest Scientific Research in the Public Welfare (China), Nos. 201404505 and 201104004.

REFERENCES CITED

Armstrong, B. T. (1978). "Wire mesh floor heating systems," *IEEE Transactions on Industry Applications* IA-14(6), 498-505.

Enríquez, E., de Frutos, J., Fernández, J. F., and de la Rubia, M. A. (2014). "Conductive coatings with low carbon-black content by adding carbon nanofibers," *Composites Science and Technology* 93, 9-16.
GB/T 9846. (2004). "Plywood," *Chinese National Standardization Management Committee*, China.
He, F. (2005). "The electrothermal property and application of carbon fiber," *New Chemical Materials* 33(6), 7-8.
Hua, Y. K., and Fu, F. (1995). "Studies on electrically conductive plywood," *Scientia Silvae Sinicae* 31(3), 254-259.
Jeon, G. W., and Jeong, G. Y. (2013). "Electric heating films based on m-aramid nanocomposites containing hybrid fillers of graphene and carbon nanotube," *Journal of Materials Science* 48(11), 4041-4049.
Khan, T. A., Gupta A., Jamari, S. S., Jose, R., Nasir, M., and Kumar, A. (2013). "Synthesis and characterization of carbon fibers and their application in wood composites," *BioResources* 8(3), 4171-4184.
Li, J. L., Xue, P., He, H., Ding, W. Y., and Han, J. M. (2009). "Preparation and application effects of a novel form-stable phase change material as the thermal storage layer of an electric floor heating system," *Energy and Buildings* 41(8), 871-880.
Lin, K. P., and Zhang, Y. P. (2003). "The performance of under-floor electric heating system with latent thermal storage," *Journal of Asian Architecture and Building Engineering* 2(2), 49-53.
Mou, Q. Y. (2007). "Experimental research on properties of heating floor with thermoelectric film," *Auhui Agricultural Science Bulletin* 13(5), 13-15.
Obata, Y., Takeuchi, K., Kawazoe, M., and Kanayama, K. (2003). "Design of functionally graded wood-based board for floor heating system with higher energy efficiency," *Materials Science Forum* 423-425, 819-824.
Qi, H. B., He, F. Y., Wan, Q. S., Li, D., and Lin, L. (2012). "Simulation analysis of heat transfer on low temperature hot-water radiant floor heating and electrical radiant floor heating," *Applied Mechanics and Materials* 204-208, 4234-4238.
Selvais, G. (2004). "Warming customers' hearts and soles' with electric floor heating," *National Floor Trends* 6(12), 52-54.
Seo, J. K., Jeon, J. S., Lee, J. H., and Kim, S. M. (2011). "Thermal performance analysis according to wood flooring structure for energy conservation in radiant floor heating systems," *Energy and Buildings* 43(8), 2039-2042.
Sun, M. Q., Mu, X. Y., Wang, X. Y., Hou, Z. F., and Li, Z. Q. (2008). "Experimental studies on the indoor electrical floor heating system with carbon black mortar slabs," *Energy and Buildings* 40(6), 1094-1100.
Wang, L. H., Peng, B., and Chen, Z. Y. (2002). "Electrothermal characteristics of cement based conductive composites," *Journal of Building Materials* 5(4), 307-310.
Yang, X. P., Rong, H. M., and Lu, Z. D. (2000). "A study of the electrical properties of carbon fiber conductive composite," *Journal of Materials Engineering* (9), 11-14.
Yuan, Q. P., Su, C. W., Huang, J. D., Gan, W. X., and Huang, Y.Y. (2013). "Process and analysis of electromagnetic shielding in composite fiberboard laminated with electroless nickel-plated carbon fiber," *BioResources* 8(3), 4633-4646.

Article submitted: May 14, 2014; Peer review completed: June 30, 2014; Revised version received and accepted: July 26, 2014; Published: July 30, 2014.